ELSEVIER

European Journal of Pharmacology 283 (1995) 207–216

ejp

Autoradiographic localization and characterization of bradykinin receptors in human skin

Elisabeth Schremmer-Danninger [a], Peter Heinz-Erian [a], Edda Töpfer-Petersen [b], Adelbert A. Roscher [a,*]

[a] *Department of Paediatrics, Section of Clinical Biochemistry, University of Munich, Munich, Germany*
[b] *Department of Dermatology, Section of Clinical Biochemistry, University of Munich, Munich, Germany*

Received 31 May 1995; accepted 7 June 1995

Abstract

High affinity [^{3}H]bradykinin binding sites have been identified in human skin cryosections by in vitro autoradiography. Equilibrium binding studies were performed with increasing concentrations of [^{3}H]bradykinin for 120 min in the presence of protease inhibitors at 4°C. In saturation experiments a single class of high affinity binding sites was identified with a dissociation constant K_d of 1.2 ± 0.8 nM (mean ± S.E.M., $n = 3$) and a maximal binding capacity B_{max} of 33 ± 8 fmol [^{3}H]bradykinin specifically bound/mg protein (mean ± S.E.M., $n = 3$). Competition experiments revealed a rank order of potency with bradykinin being most effective (bradykinin = [Lys]bradykinin > [Met-Lys]bradykinin > [Tyr]bradykinin > [des-Arg^9]bradykinin), whereas [des-Arg^9]bradykinin was ineffective. This indicates a B_2 subtype of bradykinin receptors in normal human skin. Morphological data: autoradiography revealed that bradykinin receptors were localized in the stratum basale of the epidermis. The data are consistent with the hypothesis, that these mitotic active keratinocytes express bradykinin binding sites, that fulfil the pharmacological criteria for true receptors. Diverse stimuli, including bradykinin, play a role in the mediation of cutaneous inflammatory responses (e.g. fluid extravasation, reactive cell proliferation, hyperalgesia). Our data indicate that specific kinin receptors of the stratum basale are likely to contribute to these effects.

Keywords: Autoradiography; Skin, human; Bradykinin receptor

1. Introduction

Pain and inflammation have been related to the release and action of numerous inflammatory mediators. Of these, bradykinin has drawn much attention because of its wide spectrum of pro-inflammatory pharmacology, including potent pain-producing properties, such as induction of fluid extravasation or stimulation of sensory nerve fibers (Regoli and Barabé, 1980; Steranka et al., 1988; Hargreaves and Costello, 1990).

Inflammatory reactions of the skin have been shown to be induced by many environmental stimuli including contact allergens and ultraviolet light (Proud and Kaplan, 1988; Kang-Rotando et al., 1993). It is postulated that these diverse stimuli trigger a cutaneous inflammatory response by directly inducing epidermal keratinocytes to elaborate specific proinflammatory cytokines and other mediators such as bradykinin (Barker et al., 1991). In keratinocytes bradykinin induces phosphoinositol turnover, formation of 1,2-diglyceride, tyrosine phosphorylation and cell growth (Talwar et al., 1990; Weiss and Atlas, 1991; Rosenbach et al., 1993). This is indirect evidence that kinin effects in these cells may be transmitted via specific receptors.

Recently the rat and the human B_2 subtype of the bradykinin receptor were cloned (McEachern et al., 1991; Hess et al., 1992) and by homology search this receptor was grouped to the superfamily of the G-protein-coupled seven-transmembrane receptors.

At least two, if not three types of bradykinin receptors have been postulated to exist in mammalian tissues (Bhoola et al., 1992). Only the B_2 subtype of the bradykinin receptor has been identified by receptor

* Corresponding author. Dr. von Haunersches Kinderspital, Abteilung für Klinische Biochemie, Lindwurmstraße 4, 80337 München, Germany. Fax 089/5160-4486.

Elsevier Science B.V.
SSDI 0014-2999(95)00347-9

autoradiography (Manning et al., 1986; Manning and Snyder, 1989). This method, which localizes binding sites in situ in structurally intact tissues provides an excellent means of targeting bradykinin action.

We therefore set out to identify, characterize and localize kinin receptors in the human skin using receptor-binding and autoradiographic techniques. In this report we describe the autoradiographic visualization and evaluation of some pharmacological characteristics of bradykinin binding sites in the stratum basale of the human epidermis.

2. Materials and methods

2.1. Materials

Tritium-labelled bradykinin ([2,3-prolyl-3,4-^{3}H(N)]-bradykinin) with specific activities between 78.4 and 121.6 Ci/mmol was purchased from New England Nuclear (Dreieich, Germany). Unlabelled bradykinin, [Lys]bradykinin, [Met-Lys]bradykinin were obtained from Sigma Chemie (Deisenhofen, Germany), [Tyr^8]bradykinin and bombesin were from Peninsula Laboratories (Belmont, USA, CA). Insulin like growth-factor-II was a gift from Dr. Wieland Kiess (Dept. of Pediatric Endocrinology, Dr. von Haunersches Kinderspital). All other biochemicals were obtained from Sigma Chemie (Deisenhofen, Germany). Tritium-sensitive X-ray film ([^{3}H]Hyperfilm) and photosensitive emulsion for high resolution microautoradiography (LM-1 for light microscopy) were obtained from Amersham Buchler (Braunschweig, Germany).

2.2. Tissue preparation

We obtained foreskin from healthy newborn babies undergoing elective circumcision, and histologically normal adult skin from areas surrounding dermal naevi excised for suspicion of melanoma. Tissue samples were rinsed several times in ice-cold saline and frozen immediately in liquid nitrogen. 10 or 20 μm cryostat sections were cut at -30°C and thaw-mounted on gelatine-coated slides. Sections were dried overnight in a desiccator at 4°C and either processed for immediate use or stored at -80°C. Protein content of cryosections was determined using a commercial protein microassay (Bio-Rad, Munich, Germany).

2.3. Binding studies

Gelatine-coated glass slides (Young and Kuhar, 1979) bearing 20 μm cryostat sections were temperature-equilibrated to 4°C and placed into silicon-coated polypropylene slide mailers containing 3 ml of incubation buffer. Unless stated otherwise this buffer consisted of 25 mM N-tris[hydroxymethyl]methyl-2-aminomethane-sulfonic acid (TES), 0.2% bovine serum albumine, 1 mM dithiothreitol, 10 μM captopril, 10 μM phosphoramidon, 1 μM 1.10-phenanthroline, 2 mM bacitracin and 300 mM sucrose, pH 6.8 at 4°C (Manning et al., 1989). Unless indicated otherwise 6.6 nM [^{3}H]bradykinin was added in the presence (non-specific binding) or absence (total binding) of 1 μM unlabelled bradykinin. Incubations were carried out at 4°C for 120 min. The binding reactions were terminated by washing the sections twice for 3 min at 4°C in buffer containing 25 mM TES, 0.2% bovine serum albumine, 1 mM 1.10-phenanthroline, pH 6.8 (Manning et al., 1989) to remove excess of free radioligand and dipped into ice-cold distilled water for 5 s. Sections were then immediately wiped off with filter paper and placed into liquid scintillation vials. After addition of 15 ml of scintillation fluid (Quickszint 212, Zinsser Analytic, Frankfurt, Germany) [^{3}H]radioactivity was assessed in a Beckman β-scintillation counter. Specific binding was calculated as the difference between total and non-specific binding.

2.4. Bradykinin degradation

Bradykinin degradation by incubated tissue was assessed by subjecting the incubation medium to ion exchange chromatography on CM-Sephadex C-25 in order to separate intact [^{3}H]bradykinin from degradation products of the radiolabelled tracer (Roscher et al., 1984).

2.5. Receptor autoradiography

After terminating the binding reaction cryosections were quickly dried in a stream of cold air and stored overnight in a desiccator at 4°C. The sections were then vapour-fixed with paraformaldehyde for 2 h at 80°C and defatted according to Young and Kuhar (1979).

For crude visualization and localization of [^{3}H]-bradykinin binding by macroautoradiography sections were exposed to [^{3}H]Hyperfilm (Amersham Buchler, Braunschweig, Germany) for 2–3 weeks at 4°C in X-ray cassettes.

Autoradiographs of [^{3}H]bradykinin binding were subjected to semiquantitative densitometric analysis using an Ultroscan XL laser densitometer (LKB, Bromma, Sweden).

For high resolution microautoradiography coverslips were coated with Amersham LM-1 photosensitive emulsion, carefully glued to one end of the slide and mounted to the tissue sections (Young and Kuhar, 1979). After exposure for approximately 5 weeks at 4°C the coverslips were bent away from the sections and the emulsion-autoradiographs developed. The tissue

sections were lightly stained with toluidine-blue or hematoxylin-eosin. Then the bent-away portions of the coverslips were again apposed to the slide using Eukitt mounting medium (Kindler, Freiburg, Germany). The histology of the stained sections could thus be topographically related to the silver grains on the coverslips (autoradiograph) using bright-field microscopy at 200-fold magnification.

3. Results

3.1. Binding studies

Cryosections were used to initially investigate some of the pharmacological characteristics of [^{3}H]-bradykinin binding in human skin.

Optimization of the incubation conditions

The incubation procedure was optimized with regard to inhibitors of [^{3}H]bradykinin degradation, incubation time and temperature as well as the wash protocol. Incubation of the cryosections for the period of the experiment in the standard incubation buffer containing [^{3}H]bradykinin at 4°C led to the degradation of 26% of [^{3}H]bradykinin added. This incubation medium by itself (that means without tissue sections) caused a degradation of 19% due to the albumin described as protease-free 99% (Sigma, Deisenhofen, Germany). Best results, i.e. 91% intact [^{3}H]bradykinin, were achieved by addition of 2 mM bacitracin, 10 μM captopril and 10 μM phosphoramidon to the incubation medium at 4°C. The addition of 2 mM bacitracin and 10 μM phosphoramidon alone resulted in a diminution of degradation to 11%. The further addition of the angiotensin converting enzyme inhibitor BPP9a (bradykinin potentiator 9a = SQ20881) or 1.10-phenanthroline was without effect. At 37°C 36% of [^{3}H]bradykinin were degraded within the incubation time of 120 min even with the addition of the inhibitor cocktail. The gelatine coating of the glass slides per se did not influence [^{3}H]bradykinin degradation.

If termination of the binding reaction by the wash procedure was completed within a rather short time of 3 min the best ratio between total and non-specific binding was achieved. Longer washing times up to 30

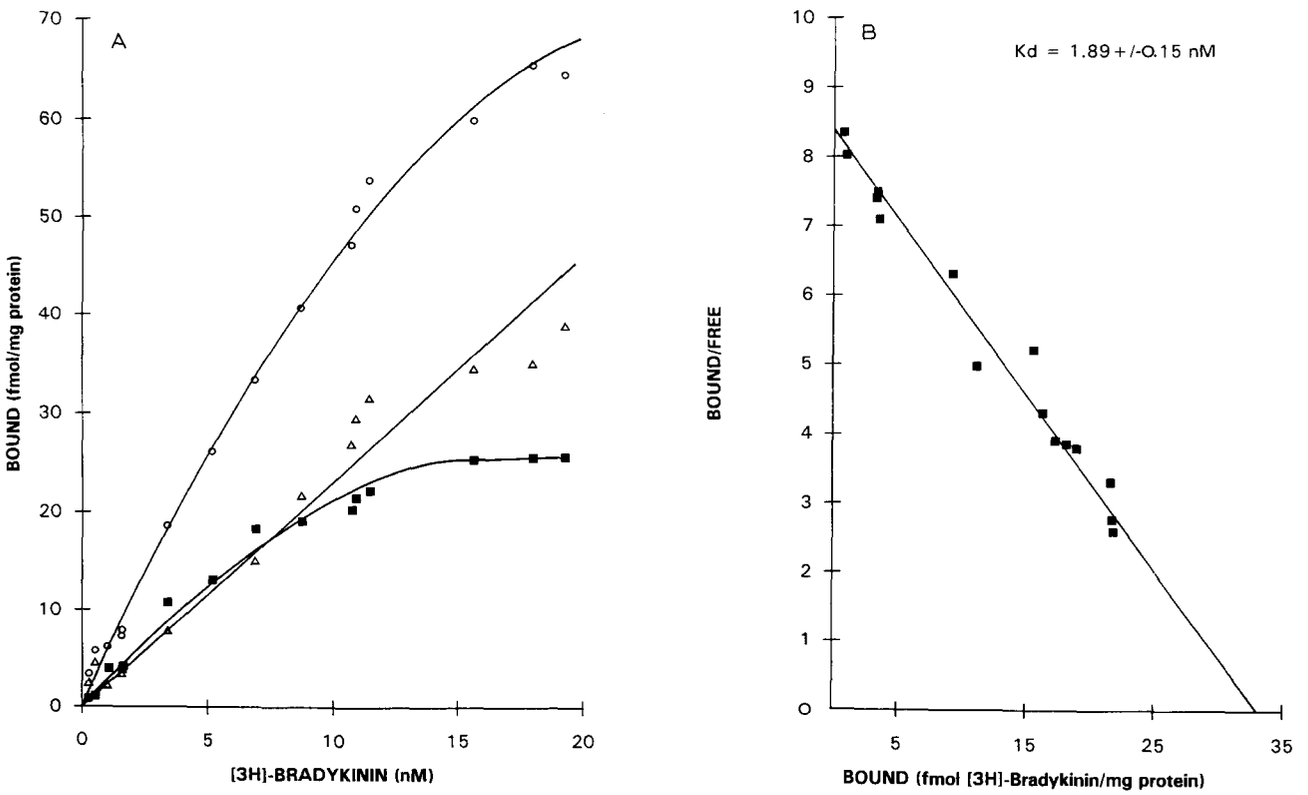

Fig. 1. Saturation curve and Scatchard analysis of [^{3}H]bradykinin binding to cryosections from newborn foreskin. (A) 20 μm Cryosections were incubated at 4°C with increasing concentrations of [^{3}H]bradykinin for 120 min in the presence or absence of 3 μM unlabelled bradykinin. The binding reaction was terminated as described in Methods. Symbols represent total (○), specific (■; i.e. total minus non-specific binding) and non-specific (△) binding. (B) Scatchard analysis of the binding results. Data points are best fitted by a straight line with a dissociation constant (K_d) of 1.89 ± 0.15 nM (mean ± S.E.M.) and a maximal binding capacity (B_{max}) of 34 ± 3 fmol [^{3}H]bradykinin specifically bound/mg protein. Data are from a representative experiment that was repeated twice with similar results. In a total of three experiments a K_d of 1.2 ± 0.8 nM and a B_{max} of 33 ± 8 fmol [^{3}H]bradykinin specifically bound/mg protein were derived.

min resulted in a further continual slow decay of both total and non-specific binding.

[^{3}H]Bradykinin equilibrium binding analysis

Equilibrium binding of [^{3}H]bradykinin to cryosections of human foreskin as a function of [^{3}H]bradykinin concentration is shown in Fig. 1. An incubation time of 120 min at 4°C was chosen to allow for complete association even at very low concentrations. Specific bradykinin binding was nearly saturated at about 12 nM [^{3}H]bradykinin. Non-specific binding was linear up to the highest concentration used (19.25 nM [^{3}H]bradykinin). Scatchard analysis of these data revealed a single class of binding sites with a K_d of 1.89 ± 0.15 nM and B_{max} of 34 ± 3 fmol [^{3}H]bradykinin specifically bound/mg protein. In a total of three experiments a K_d of 1.2 ± 0.8 nM and a B_{max} of 33 ± 8 fmol [^{3}H]bradykinin specifically bound/mg protein were derived. In an experiment using adult skin maximal binding capacity of 110 ± 12 fmol [^{3}H]bradykinin specifically bound/mg protein and a K_d of 1.87 ± 0.54 nM were shown.

Association and dissociation kinetics of [^{3}H]bradykinin binding to cryosections of human foreskin

In Fig. 2 the association of [^{3}H]bradykinin at 4°C to cryosections of foreskin at a concentration of 6.6 nM [^{3}H]bradykinin and the subsequent dissociation after addition of 3 μM unlabelled bradykinin are shown. Equilibrium was obtained within 70 min of association and remained rather constant for the following 75 min. Dissociation was initiated after 120 min of association by direct addition of 3 μM unlabelled bradykinin and resulted in an exponential reduction of specifically bound [^{3}H]]bradykinin.

The data of these experiments were analyzed according to the following pseudo-first order equation:

$$Bt = Beq(1 - \exp[k_{obs}(-t)]),$$

where k_{obs} is the observed pseudo-first order rate constant of association, Beq the amount of maximum specific binding at equilibrium (expressed as 100% binding) at a given ligand concentration, and Bt the percentage of Beq at time t. From the pseudo-first order semilogarithmic plot of the association data a k_{obs} of 0.0262 min^{-1} was obtained. From the first-order rate semilogarithmic plot of the dissociation of the receptor-ligand complex the slope of the line, k_d, determined by linear regression analysis was equal to the first-order rate dissociation constant $k_d = -0.0037 \pm 0.001$ min^{-1}. The negative value indicates the reversibility of the reaction.

The second-order rate constant of radioligand association k_a was estimated from the equation

$$k_{obs} = k_a([^3\text{H}]\text{bradykinin}) + k_d,$$

and was $k_a = 0.0018 \pm 0.0004$ nM^{-1} min^{-1}.

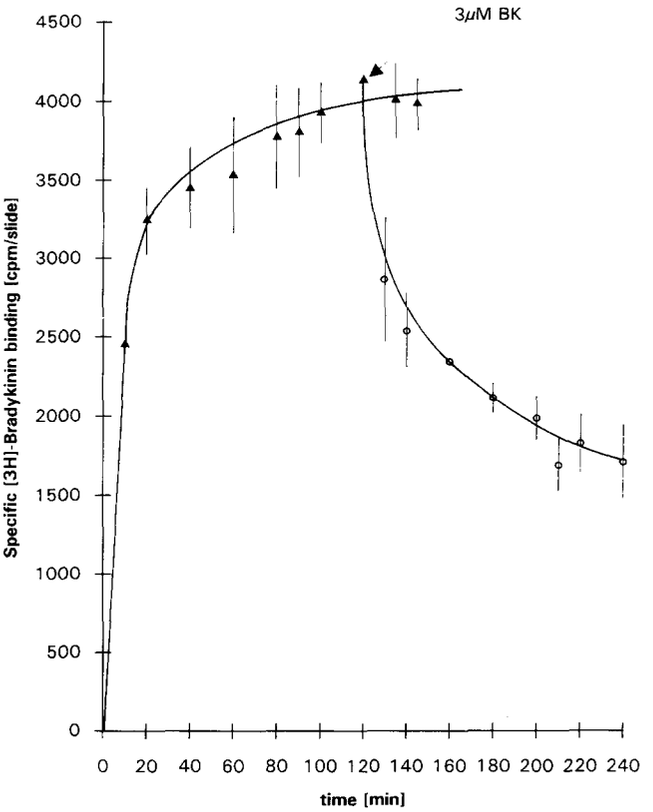

Fig. 2. Association and dissociation kinetics of [^{3}H]bradykinin binding. To investigate the association of [^{3}H]bradykinin, 20 μm cryosections of foreskin were incubated at 4°C in buffer with 6.6 nM [^{3}H]bradykinin as described. Specific [^{3}H]bradykinin binding was measured at the times indicated (▲). Dissociation was initiated after 120 min of association by addition of 3 μM unlabelled bradykinin (○). Symbols represent the mean ± S.D. of duplicate determinations.

Finally the equilibrium dissociation constant $K_d = k_d/k_a$ was calculated from these kinetic parameters giving a value of 2.05 ± 0.7 nM, which was in good agreement with the mean equilibrium dissociation constant K_d of 1.2 ± 0.8 nM obtained from three different equilibrium binding experiments.

Specificity of [^{3}H]bradykinin binding to cryosections of human foreskin

Different bradykinin analogs and various unrelated peptides such as bombesin and insulin like growthfactor-II were tested for their potency to compete with [^{3}H]bradykinin for binding to cryosections of human foreskin (Table 1). The following rank order of potencies compatible with a B_2 receptor subtype was obtained: bradykinin = [Lys]bradykinin > [Met-Lys]bradykinin > [Tyr]bradykinin > [des-Arg^9]bradykinin. Bombesin and insulin like growthfactor-II were ineffective in displacing [^{3}H]bradykinin binding to human skin.

3.2. Localization of [^{3}H]bradykinin binding sites in human skin by film autoradiography

Autoradiography revealed specific [^{3}H]bradykinin binding sites over discrete portions in cryosections of both adult human skin (Fig. 3) and newborn foreskin (Fig. 4). Relating the film autoradiographs to the histology of the cryosections resulted in the identification of the epidermis as the site of tracer binding. On densitometric analysis specific binding was determined to be 56.3% (derived from table in Fig. 3C, *heights*) and 51.15% (derived from table in Fig. 3C, *areas*) for

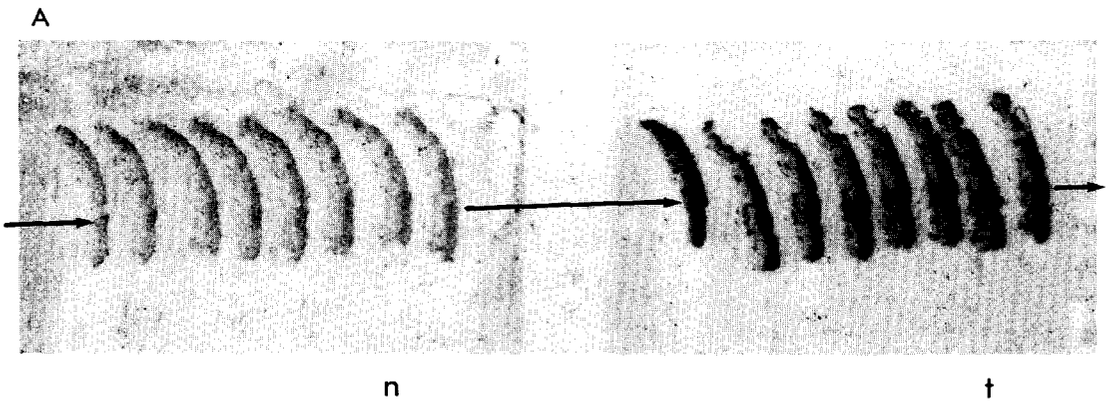

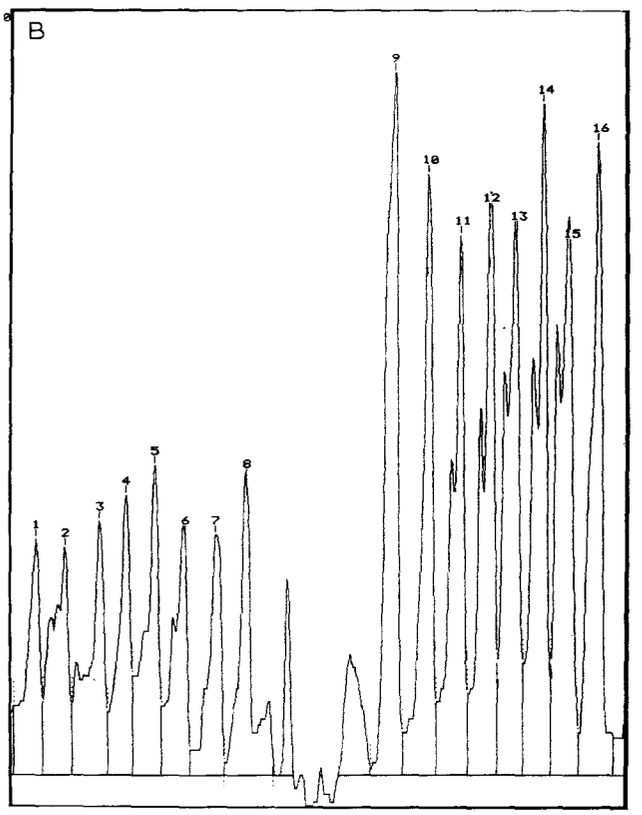

C

Peak No.	Height (AU)	Area (AU*mm)
Optical density: Nonspecific binding		
1	0.091	0.12624
2	0.088	0.14880
3	0.098	0.16016
4	0.108	0.12984
5	0.120	0.16032
6	0.093	0.13384
7	0.093	0.11880
8	0.115	0.15280
Mean ± S.D.	0.10075 ± 0.01124	0.14135 ± 0.01511
Optical density: Total binding		
9	0.271	0.31800
10	0.232	0.24200
11	0.208	0.25296
12	0.217	0.28904
13	0.210	0.29744
14	0.259	0.31248
15	0.203	0.31768
16	0.244	0.28480
Mean ± S.D.	0.2305 ± 0.0237	0.28930 ± 0.02695

Fig. 3. Autoradiographic localization of [^{3}H]bradykinin binding sites in adult human skin. Tritium-sensitive film was used as described in Methods. (A) Macroautoradiograph of cryosections from adult human skin showing total binding (t, right panel) and non-specific binding (n, left panel). (B) Analysis of the autoradiographs shown in Fig. 3A by laser densitometry. Mean optical density (OD) of 'non-specific binding' autoradiographs (left panel) was 43.7% and 48.85% of that in 'total binding' autoradiographs, leaving 56.3% and 51.15% specific binding (derived from the amounts of *heights* and *areas*). Original length of a cryosection was 0.8 cm. (C) Table of optical density of defined peaks of the upper laser densitometry shown as *heights* and *areas*.

adult skin sections (Fig. 3), in foreskin from newborn babies (Fig. 4) specific binding (total binding minus non-specific binding) was 33.14% (derived from table in Fig. 4C, *heights*) and 47.65% (derived from table in Fig. 4C, *areas*).

3.3. Localization of [^{3}H]bradykinin binding sites in human skin by emulsion autoradiography

Autoradiograph using emulsion-coated coverslips revealed silver grains in high densities over the stratum

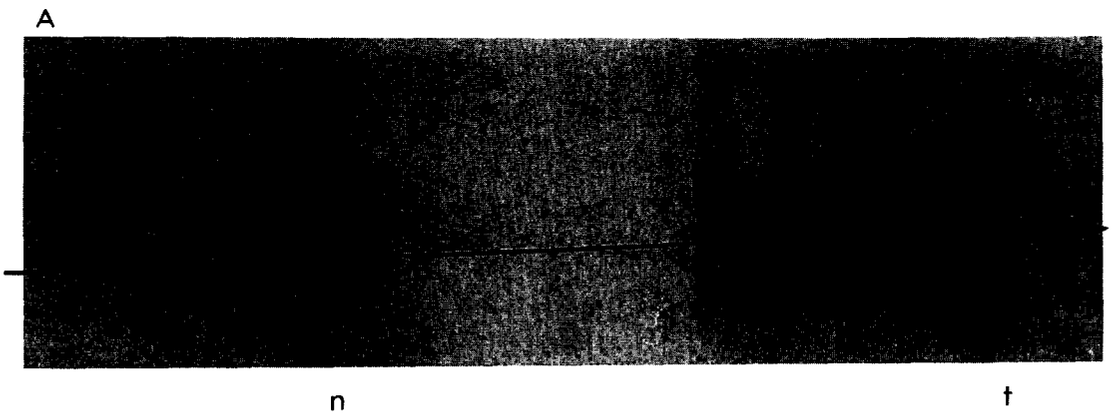

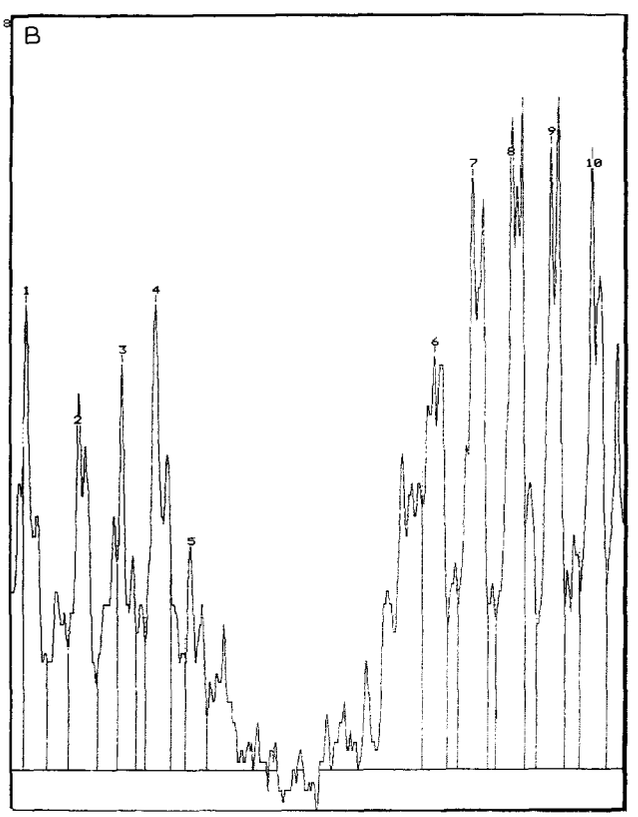

C

Peak No.	Height (AU)	Area (AU*mm)
Optical density: Nonspecific binding		
1	0.115	0.15448
2	0.083	0.16296
3	0.100	0.11256
4	0.115	0.18920
5	0.053	0.07896
Mean ± S.D.	0.0932 ± 0.0233	0.13963 ± 0.03907
Optical density: Total binding		
6	0.102	0.21568
7	0.146	0.28720
8	0.149	0.30464
9	0.154	0.27400
10	0.146	0.25208
Mean ± S.D.	0.1394 ± 0.0189	0.26672 ± 0.03075

Fig. 4. Autoradiographic localization of [^{3}H]bradykinin bindig sites in human newborn foreskin. Tritium-sensitive film was used as described in Methods. (A) Macroautoradiograph of cryosections from human newborn foreskin showing total binding (t, right panel) and non-specific binding (n, left panel). (B) Analysis of the autoradiographs shown in Fig. 4A by laser densitometry. Mean optical density (OD) of 'non-specific binding' autoradiographs was 66.86% and 52.35% of that in 'total binding' autoradiographs, leaving 33.14% and 47.65% specific binding (derived from the amounts of *heights* and *areas* of the following table). Original length of a cryosection was 1 cm. (C) Table of optical density of defined peaks of the laser densitometry (Fig. 4B) shown as *heights* and *areas*.

Table 1
Relative potencies of bradykinin analogues and unrelated peptides in competing with [^{3}H]bradykinin binding to cryostat sections of human foreskin

	K_i	Relative affinity
Bradykinin	2.4×10^{-9}	100%
[Lys]bradykinin	3.1×10^{-9}	75%
[Met-Lys]bradykinin	6.3×10^{-9}	43%
[Tyr]Bradykinin	7.4×10^{-9}	40%
[des-Arg^9]bradykinin	2.5×10^{-6}	2%
Bombesin	–	< 0.5%
Insulin-like growth factor II	–	< 0.5%

K_i values were calculated by the equation outlined by Cheng and Prusoff (1973). Sections were incubated with 3.6 nM [^{3}H]bradykinin and with increasing concentrations of unlabelled peptides (10^{-11} M to 10^{-6} M) for 120 min at 4°C. Specific binding was determined as described in Methods. To determine potencies, six concentrations of each peptide were assayed in duplicates.

basale of the epidermis and the lowest layer of the stratum spinosum (Fig. 5A, adult skin and Fig. 5D, newborn foreskin). Control sections, incubated in the same buffer but with an excess of unlabelled bradykinin contained only diffusely scattered silver grains with no preference for a distinct tissue structure (Fig. 5B, adult skin and Fig. 5E, newborn foreskin), thus demonstrating the specificity of [^{3}H]bradykinin binding to the basal layers of the epidermis. This mitotically active area of the epidermis, the stratum basale, consists of undifferentiated keratinocytes. Closer to the surface of the skin with increasing differentiation of keratinocytes in the stratum spinosum, stratum granulosum and stratum corneum an increase of keratin content is observed (Fig. 5C). In the section shown in this figure keratinocytes were stained using the anticytokeratin antibody KL 1 (Boehringer, Mannheim, Germany). Due to its higher keratin content the horny layer looks darker than the non-differentiated keratinocytes in the stratum basale. Fig. 5F shows a section of newborn foreskin which was stained with toluidine-blue. In adult skin total [^{3}H]bradykinin binding was more intense as compared to newborn foreskin and this was also reflected by a higher B_{max} of specific binding of this tissue.

4. Discussion

This study shows that specific bradykinin receptors of the B_2 subtype are present throughout the stratum basale of the epidermis in both adult skin and foreskin of newborn babies. The demonstration of the existence of bradykinin binding sites in the human epidermis is based on several experimental grounds. First, in competitive binding studies using cryostat sections from human skin the site labelled by [^{3}H]bradykinin clearly preferred bradykinin and [Lys]bradykinin over [Met-Lys]bradykinin, [Tyr]bradykinin, [des-Arg^9]bradykinin in this rank order and did not recognize bombesin or insulin like growth factor-II. This is in good agreement with the specificity to be expected of a B_2 subtype of the bradykinin receptor. Second, in saturation experiments the resulting Scatchard plots yielded a single class of high affinity binding sites with a dissociation constant (K_d) of 1.89 ± 0.15 nM. Two further similar experiments showed K_d values of 0.9 ± 0.37 nM and 1.0 ± 0.52 nM. Therefore the $K_d \pm$ S.E.M. resulted in 1.2 ± 0.8 nM. Third, association kinetics revealed that a binding equilibrium was reached under conditions that compared well to those described for other tissues tested (Roscher et al., 1983). In addition, dissociation kinetics showed that binding was rapidly reversible. Taken together, characteristics of [^{3}H]bradykinin binding showed a specificity, saturability and kinetics consistent with true receptor binding.

The degradation of [^{3}H]bradykinin by the tissue sections observed in initial experiments indicated that it was necessary to add enzyme inhibitors to the incubation and wash media. The major bradykinin degrading enzyme in human fibroblasts appears to be the membrane-bound neutral endopeptidase-24.11 (Lorkowski et al., 1987). In human skin sections we observed that the major portion of bradykinin degrading activity was inhibited by phosphoramidon, a very potent inhibitor of neutral endopeptidase-24.11, whereas captopril as the inhibitor of angiotensin I converting enzyme had only little effect. In addition, bacitracin (Roscher et al., 1983) and 1.10-phenanthroline were added to prevent non-specific degradation caused by albumin solutions. Neutral endopeptidase-24.11 is the major bradykinin degrading enzyme in human skin.

A major goal of this study was to localize bradykinin receptors in the human skin. Macroautoradiography, using tritium-sensitive film demonstrated that specific [^{3}H]bradykinin binding sites were localized within the epidermis. In microautoradiograms the distribution of these epidermal [^{3}H]bradykinin binding sites was shown to be localized predominantly over the stratum basale of the epidermis of both newborn foreskin and adult skin. This suggests a direct involvement of bradykinin in the physiology of epidermal mitotically active cells and supports the idea of bradykinin as a mitogenic agent recently discussed by several authors (Goldstein and Wall, 1984; Talwar et al., 1990). In this context it may be interesting to note that preliminary experiments in our laboratory with monolayers of cultured keratinocytes have shown that additon of 200 nM bradykinin reduces the time necessary to reach confluency (E.S.-D., personal observation).

Enhanced release of bradykinin has been demon-

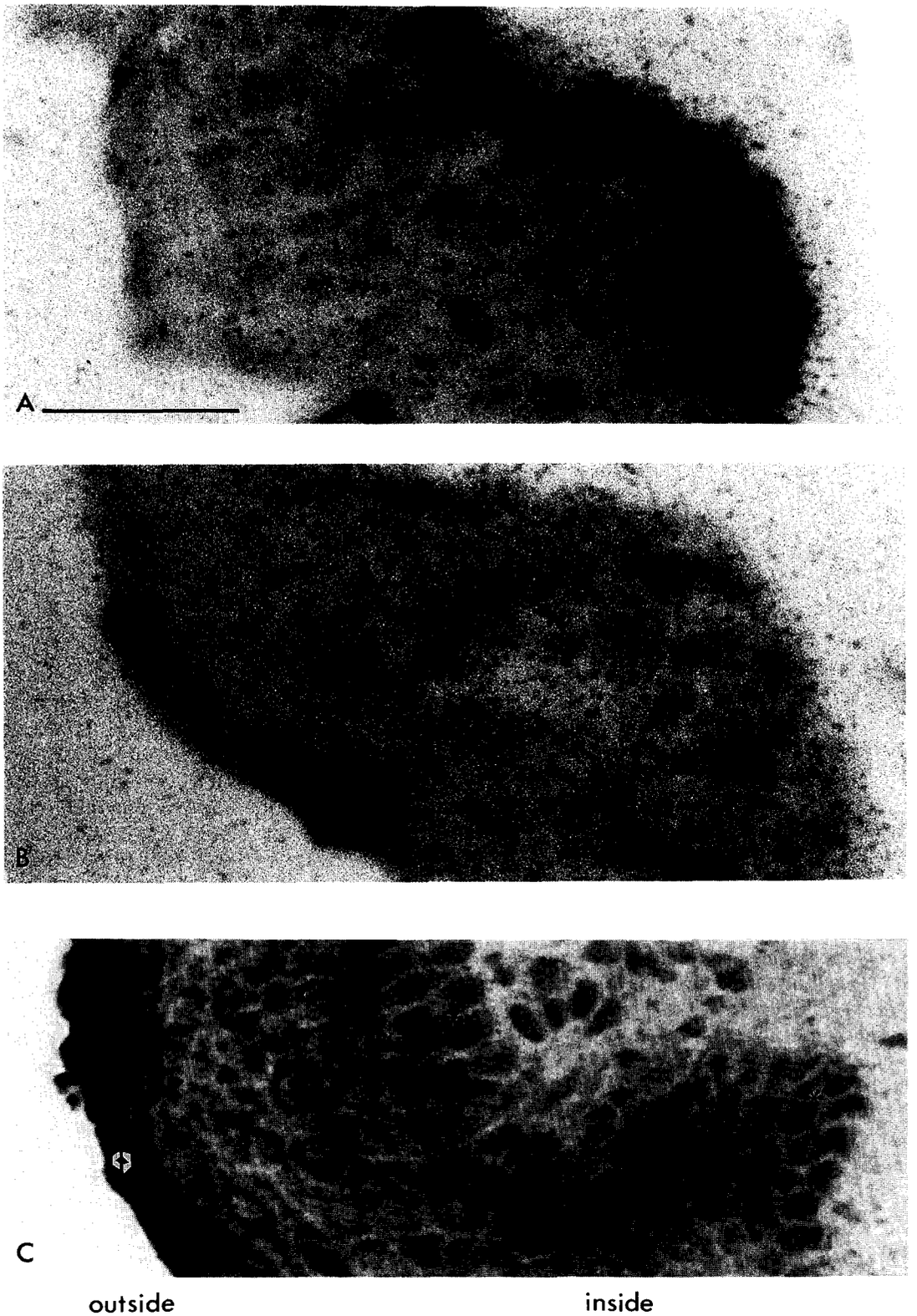

Fig. 5. Distribution of [^{3}H]bradykinin binding sites in adult human skin and in newborn foreskin as detected by autoradiography. Emulsion-coated coverslips were used as described in Methods. Adult human skin (A–C); newborn foreskin (D–F). (A,D) Microautoradiograph of total binding (= incubation with 3 nM [^{3}H]bradykinin) shows intense labelling over the stratum basale of the epidermis with few silver grains over the other cell layers of the skin. (B,E) Microautoradiograph of non-specific binding (= 3 nM [^{3}H]bradykinin in the presence of 3 μM unlabelled bradykinin). Only a few silver grains are scattered over the whole epidermis without any specific preference for a certain cell layer. (C) Toluidine-blue- and KL 1-stained cryostat section of epidermis. (*) Stratum basale, (○) stratum spinosum, (▽) stratum granulosum, (◇) stratum corneum. (F) Toluidine-blue-stained cryostat section of epidermis. Length of calibration bar is 50 μm.

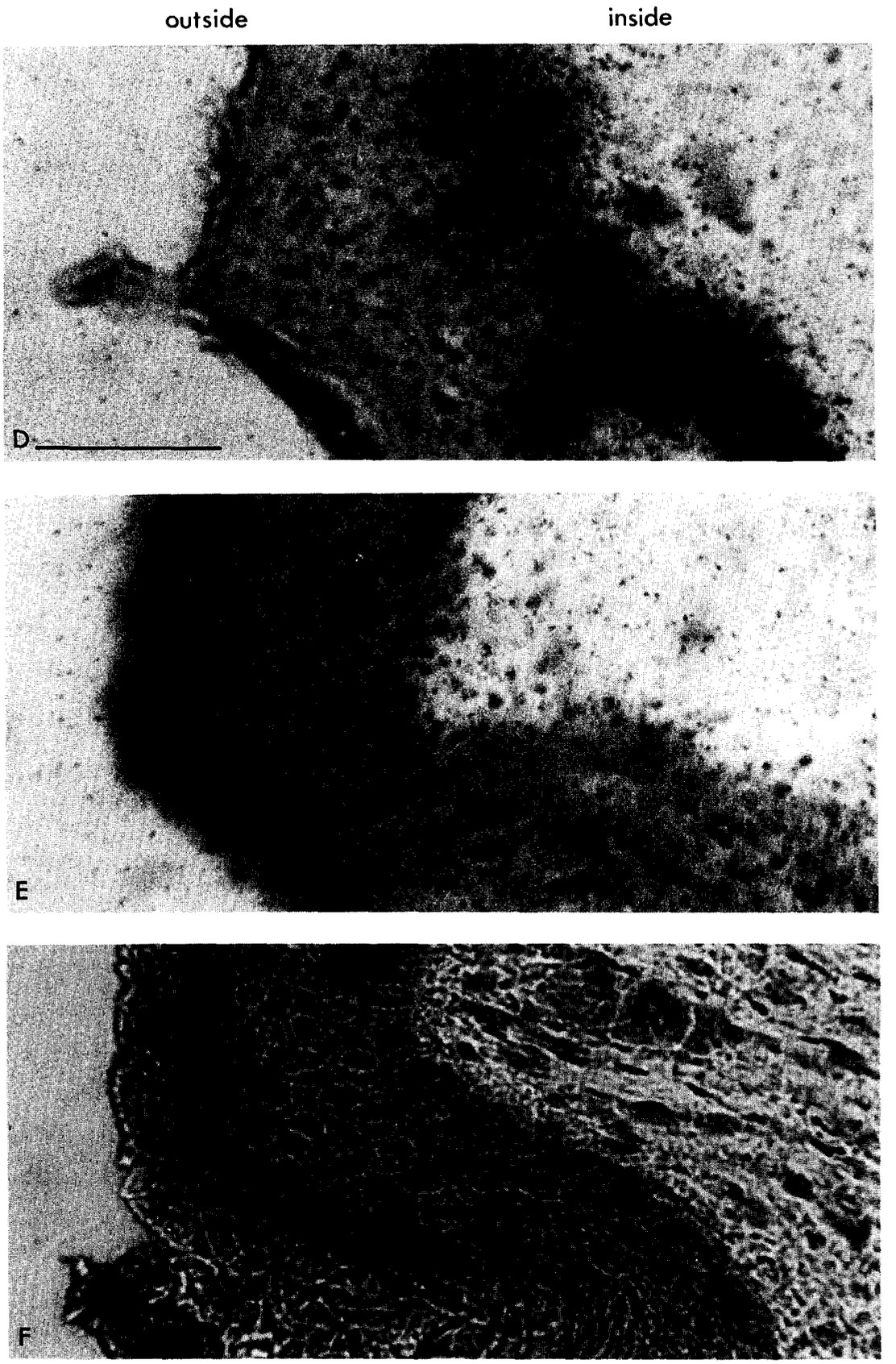
outside
inside
D
E
F

strated in inflammatory processes (Hargreaves and Costello, 1990). It has, therefore, been hypothesized that the tissue proliferation after the onset of inflammatory reactions may be caused in part by bradykinin. Kimball and Fisher (1988) reported that bradykinin potentiates enhanced proliferation of 3T3 fibroblasts due to interleukin-1. Proliferation of these cells was also increased, although to a lower degree, when the mediators were tested individually. This concerted action of these two different inducers of inflammation indicates that bradykinin may exert a moderate but important promotor effect during inflammatory reactions in the skin.

Interleukin-1 is reported to potentiate bradykinin- and tumor necrosis factor-induced prostaglandin E_2 release (O'Neill and Lewis, 1989).

These observations may provide a pathophysiological concept for the potential contribution of bradykinin, kinin receptors and cytokines during inflammatory reactions of the skin.

In conclusion, we have been able to demonstrate specific bradykinin B_2 receptor-binding sites in the basal layers of the human epidermis. The fact that these sites are very specifically confined to skin tissue of high mitotic activity suggests that bradykinin may play an important role in epidermal cell proliferation.

Acknowledgements

This work was supported by a grant of the 'Sonderforschungsbereich 207', project F4, of the University of Munich.

References

Barker, J.N.W.N., R.S. Mitra, C.E.M. Griffiths, V.M. Dixit and B.J. Nickoloff, 1991, Keratinocytes as initiators of inflammation, Lancet 337, 211.

Bhoola, K.D., C.D. Figueroa and K. Worthy, 1992, Bioregulation of Kinins: Kallikreins, Kininogens and Kininases, Pharmacol. Rev. 44, 1.

Cheng, Y.-C. and W.H. Prusoff, 1973, Relationship between the inhibition constant (K_i) and the concentration of inhibitor which causes 50 percent inhibition (IC_{50}) of an enzymatic reaction, Biochem. Pharmacol. 22, 3099.

Goldstein, R.H. and M. Wall, 1984, Activation of protein formation and cell division by bradykinin and [des-Arg^9]bradykinin, J. Biol. Chem. 259, 9263.

Hargreaves, K.M. and A. Costello, 1990, Glucocorticoids suppress levels of immunoreactive bradykinin in inflamed tissue as evaluated by microdialysis probes, Clin. Pharmacol. Ther. 48, 168.

Hess, J.F., J.A. Borkowski, G.S. Young, C.D. Strader and R.W. Ransom, 1992, Cloning and pharmacological characterization of a human bradykinin (BK-2) receptor, Biochem. Biophys. Res. Commun. 184, 260.

Kang-Rotando, C.H., C.C. Miller, A.R. Morrison and A.P. Pentland, 1993, Enhanced keratinocyte prostaglandin synthesis after UV injury is due to encreased phospholipase activity, Am. J. Physiol. 264, C 396.

Kimball, E.S. and M.C. Fisher, 1988, Potentiation of IL-1-induced Balb/3T3 fibroblasts proliferation by neuropeptides, J. Immunol. 141, 4203.

Lorkowski, G., J.E. Zijderhand-Bleekemolen, E.G. Erdös, K.V. Figura and A. Hasilik, 1987, Neutral endopeptidase 24.11 (enkephalinase), Biochem. J. 248, 345.

Manning, D.C. and S.H. Snyder, 1989, Bradykinin receptors localized by quantitative autoradiography in kidney ureter and bladder, Am. J. Physiol. 256, F909.

Manning, D.C., R. Vavrek, J.M. Stewart and S.H. Snyder, 1986, Two bradykinin binding sites with picomolar affinities, J. Pharmacol. Exp. Ther. 237, 504.

McEachern, A.E., E.R. Shelton, S. Bhakta, R. Obernolte, Ch. Bach, P. Zuppan, J. Fujisaki, R.W. Aldrich and K. Jarnagin, 1991, Expression cloning of a rat B2 bradykinin receptor, Proc. Natl. Acad. Sci. USA 88, 7724.

O'Neill, L.A.J. and G.P. Lewis, 1989, Interleukin-1 potentiates bradykinin-and TNF-induced PGE2 release, Eur. J. Pharmacol. 166, 131.

Proud, D. and A.P. Kaplan, 1988, Kinin formation: mechanisms and role in inflammatory disorders, Ann. Rev. Immunol. 6, 49.

Regoli, D. and J. Barabé, 1980, Pharmacology of bradykinin and related kinins, J. Pharmacol. Rev. 32, 1.

Roscher, A.A., V.C. Manganiello, C.L. Jelsema and J. Moss, 1983, Receptors for Bradykinin in intact cultured human fibroblasts, J. Clin. Invest. 72, 626.

Roscher, A.A., V.C. Manganiello, C.L. Jelsema and J. Moss, 1984, Autoregulation of bradykinin receptors and bradykinin-induced prostacyclin formation in human fibroblasts, J. Clin. Invest. 74, 552.

Rosenbach, T., C. Liesegang, S. Binting and B.M. Czarnetzki, 1993, Inositol phosphate formation and release of intracellular free calcium by bradykinin in HaCaT keratinocytes, Arch. Dermatol. Res. 285 (7), 393.

Steranka, L.R., D.C. Manning, Ch.J. DeHaas, J.W. Ferkany, S.A. Borosky, J.R. Connor, R.J. Vavrek, J.M. Stewart and S.H. Snyder, 1988, Bradykinin as a pain mediator: Receptors are localized to sensory neurons and antagonists have analgesic actions, Proc. Natl. Acad. Sci. USA 85, 3245.

Talwar, H.S., G.J. Fisher and J.J. Voorhees, 1990, Bradykinin induces phosphoinositide turnover, 1,2-diglyceride formation and growth in cultured adult human keratinocytes, J. Invest. Dermatol. 95, 705.

Weiss, C. and D. Atlas, 1991, The bradykinin receptor – a putative receptor-operated channel in PC12 cells: studies of neurotransmitter release and inositol phosphate accumulation, Brain Res. 543, 102.

Young, W.S. and M.J. Kuhar, 1979, A new method for receptor autoradiography: [^{3}H]opioid receptors in rat brain, Brain Res. 179, 25.